Paul Szelemej

VDAC and BNIP3: A Crucial Interaction's Role in Delayed Neuronal Cell Death in Stroke

Student: Mr. Paul Szelemej **Supervisor:** Dr. Jiming Kong

Departmental Affiliation: Department of Human Anatomy and Cell Science, Faculty of Medicine, University of Manitoba

Summary: Stroke is currently the third leading cause of death, and the leading cause of disability in Canada. In a stroke, the majority of neuron death is due to apoptosis triggered by stress from the ischemic insult. In theory, this means that those cells are not predestined to die, but rather program themselves to do so, making understanding apoptotic pathways crucial for potential therapeutic interventions in the future. Although there are countless apoptotic mechanisms and pathways, one important, caspase-independent pathway is that of BNIP3, a death inducing mitochondrial protein. It is currently known that BNIP3 somehow inserts into the mitochondrial membrane, and facilitates the mitochondrial release of apoptotic factors like Endonuclease G and Apoptosis Inducing Factor (AIF), thus further continuing the self-destruction of the cell. Our hypothesis is that the intermediate through which BNIP3 binds and communicates its pro-apoptotic message is VDAC (Voltage Dependent Anion Channels). This hypothesis is based on previous work showing a strong interaction between VDAC and BNIP3 using coimmunoprecipitation and GST pull-down assay techniques. The relationship between BNIP3 and Endo G release with/without VDAC inhibition in murine mitochondria was studied, and the preliminary results support the hypothesis, as EndoG release was significantly decreased upon inhibition of the VDAC receptors in fresh mitochondria, thus implying that VDAC is a significant intermediary between BNIP3 and EndoG in this apoptotic cascade. This could potentially have tremendous therapeutic implications for the future, in which one might be able to minimize apoptotic neuronal loss after suffering a stroke, through the inhibition of VDAC.

Acknowledgements: The stipendiary support for the B. Sc. (Med) student was provided entirely or in part by the H.T. Thorlakson Foundation, Faculty of Medicine Dean, St. Boniface Research Foundation, Manitoba Health Research Council, Manitoba Institute of Child Health, Kidney Foundation of Manitoba, Leukemia and Lymphoma Society of Canada, CancerCare Manitoba, Manitoba Medical Services Foundation, Faculty of Medicine Associate Dean (Research), Heart and Stroke Foundation, and Health Sciences Centre Research Foundation; of which all sponsors are gratefully acknowledged. Dr. Kong's research is supported by a grant from the Canadian Stroke Network. The author would also like to thank Dr. Kong, Ruoyang Shi, Jiequin Weng, and all other colleagues in the laboratory for their ongoing support, encouragement, and guidance.

Student's Signature

Supervisor's Signature

Paul Szelemej

Introduction

Stroke is currently the third-leading cause of death in Canada (~7% of all deaths), and the primary cause of disability, wreaking havoc on many Canadian families every day. When a stroke occurs, there is a cessation of blood flow to the given, now ischemic area of the brain[1], which typically creates an acute infarct core (completely starved of oxygen/nutrients, it consists of a relatively instant mass of dying neurons due to direct hypoxia), and a penumbra (with partial hypoxemia), a neighbouring region of neurons around the core that die in the coming hours to days, even if reperfusion of infracted area is established[2]. It is this key phenomenon of "delayed neuronal death" in strokes that is currently the primary target for prospective neuroprotective strategies. The pro-apoptotic BNIP3 gene has recently been shown to activate a novel, caspase-independent cell death pathway (see Fig.1) that has been implicated in delayed neuronal death (classical apoptosis pathways are commonly caspase-dependent)[2,3]. BNIP3 protein dimerizes, somehow translocates into the mitochondrial membrane, and stimulates the release of apoptogenic factors like Endo G and AIF, which then migrate to the nucleus, and destroy DNA, ultimately shutting down the cell. Although VDAC's role in the well-described phenomenon of mPTP formation (mitochondrial permeability transition pore whose formation leads to loss of the $\Delta\psi_m$ gradient(mitochondrial membrane potential) in apoptosis is rather controversial[24] (with strong evidence that it is not required for mPTP formation in VDAC knockout studies), it is indubitably clear that VDAC overexpression is involved with $\Delta\psi_m$ collapse, radical oxygen species (ROS) production/release, and apoptosis[5], possibly through pore formation[6].

As for BNIP3, it is hitherto the only "death-inducing" gene that shows a characteristically delayed expression pattern in strokes[2,4], as is clearly demonstrated in Fig. 2. It has several domains, the most common of which are the PEST, BH3, transmembrane (TM), and CD domains (see Fig. 2). Any of the domains could theoretically be involved with the proposed physiological BNIP3/VDAC protein interaction, despite current evidence only existing for TM domain interactions, which is why it is currently our hypothesized primary suspect for BNIP3's key component through which it binds to VDAC. Preliminary data from the laboratory has shown that inhibition of BNIP3 expression indeed protects a very substantial 90% of neurons in culture from delayed cell death induced by oxygen-glucose deprivation for three hours. Furthermore, through co-immunoprecipitation and GST pull-down assay experiments, there is compelling evidence that BNIP3 interacts with mitochondria through binding to their voltage-gated anion channels (VDAC), which have numerous unrelated functions within the outer mitochondrial membrane. The hypothesis is that through interactions with VDAC[5], and the subsequent release of death-inducing proteins[4], BNIP3 is a regulator of delayed neuronal death in stroke.

Therefore, in theory, blocking the BNIP3 pathway should protect neurons from death, and minimize neurological deficits in victims after a stroke. My objectives in this project are to determine: the extent to which VDAC is involved with BNIP3-induced mitochondrial permeabilization, which specific motif of BNIP3[16] interacts with VDAC, and the biological function therein. If these objectives can demonstrate support for the hypothesis, testing of other inhibitors' (such as Necrostatin-1) effectiveness in blocking[7] the VDAC/BNIP3 interaction in vivo would be initiated, to be followed by live murine MCAO (Middle Cerebral Artery Occlusion) stroke models being administered potential VDAC inhibitors, thus further studying

the same relationships in a live model. More plasmids would be made to express specific amino acid mutations, in order to investigate and better pinpoint what part of the BNIP3 polypeptide interacts. The insights to be gained through the understanding of this interaction are invaluable as, in theory, new and monumental neuroprotective strategies could be clinically implemented in the bedside care of stroke victims, significantly minimizing the extent of their disability, suffering, and life lost.

Materials and Methods

For a complete description detailing the solutions used throughout the course of these experiments, please refer to Table 1.

Cell Culture

An SY5Y human neuroblastoma cell line was cultured in six-well plates incubated at 37˚C using high-glucose complete DMEM medium, and exposed to oxygen and glucose deprivation (OGD) in a hypoxic chamber in EBSS medium for six hours. With a control set, the cells were reperfused by replacing the EBSS with the complete DMEM medium and placed back in a normoxic chamber (regular culturing conditions) for 24, 48, and 72 hours. During repassaging of generations, a 0.25% trypsin solution was applied for 2 minutes with 37˚ heat for removal, and PBS was used for rinsing. Once the control and treated cell samples were obtained, they were lysed with lysis buffer and microcentrifuged at 5000 and 20000 rpm for five minutes each using a Thermo Scientific mitochondrial separation kit, being separated into corresponding cytosolic, nuclear, and mitochondrial supernatants. Samples were now ready for Western Blot analysis.

Synthesis, Preparation, and Optimization of VDAC Inhibitors for the Experiments

Dextran T70, König's polyanion, Ruthenium Red, and phosphorothioate 18-mer oligonucleotides were chosen as VDAC inhibitors for this study as they all had good literature supporting their use in VDAC inhibition, each with unique benefits, as can be seen in Table 2. Ruthenium Red, Dextran T70, and the phosphorothioate oligonucleotide randomers were all prepared in their correspondingly appropriate buffers at a concentration slightly higher than their optimum (as dilution would occur when put in for mitochondrial incubation). König's polyanion had to be synthesised de novo from methacrylic acid, maleic acic anhydride, and styrene in toluene at 60˚C. It turns out that that just over 60˚C, an irreversible, extremely exothermic reaction occurs. Thus significant time was spent optimizing conditions attainable in the laboratory that would create the product without the undesired explosive and useless reaction that occurs otherwise (the method ultimately used can be seen in Table 1). Once all of the inhibitors were in place, numerous optimization studies were done, finding the minimum concentration of each of the inhibitors needed to display VDAC inhibition as shown by EndoG/AIF release after mitochondrial incubation with the BNIP3 and BNIP3ΔTM proteins. Details regarding the mitochondrial isolation and incubation follow in a subsequent section.

Paul Szelemej

Transformation and Culturing of Bacteria

Competent DHF-α E. coli cells were melted on ice, and 50 µL of cells were placed into autoclaved tubes with 10 ng of the given plasmid of interest containing the desired GST fusion protein gene (pGEX-4T-1, see Fig. 3). Incubation on ice took place for 30 minutes, followed by a 45 second heat shock at 42˚C. The tubes were again incubated on ice for 2 minutes, prior to having 0.95 mL of LB medium added into each tube. Incubation now took place at 37˚C for 90 minutes. 100 µL of transformed cells were plated onto LB agar plates with ampicillin. As the plasmid in question imparts ampicillin resistance on the E. coli, successfully transformed bacteria should have no difficulty growing on the plate. After 16 hours of incubation at 37˚C, individual colonies were observed the next day. A single colony of each transformed type was put into sterile 10 mL tubes with 4mL of LB solution (with Ampicillin) for further incubation at 37˚C with 250 rpm turbulence overnight. This was repeated again on a larger scale, with the 4 mL of clonal E. coli from the single colony put into 200 mL of LB Amp^+ medium in an Erlenmeyer flask for shaking at 37˚C overnight. The cells were then centrifuged into pellets and underwent DNA extraction using a "Qiagen Plasmid Plus Maxi" DNA extraction kit according to their protocol. Spectrophotometry was used to determine the concentration of plasmids in the final eluting buffer.

Restriction Enzyme Analysis and DNA Electrophoresis

pGEX-4T-1 plasmids (containing the DNA sequence for GST-BNIP3 and GST-BNIP3ΔTM) were diluted to a common concentration of 0.03 µg/µL as determined by a NanoVue Plus spectrophotometer at a 280/260 nm absorbance ratio. 7 µL samples were then mixed with specific restriction endonucleases and their corresponding buffered reagents. 1 µL of NE Reagent III, 1 µL of BamHI, and 1 µL of NotI were added to the plasmid solution in order to make 10 µL aliquots, while control aliquots had 2 µL of ddH_2O added instead of the enzymes. All were then incubated in a water bath at 30˚C (NotI optimum temperature), and 37˚C (for BamHI) for an hour each. GelRed was added (in a 1:5 ratio) to the digested plasmid solutions, and 5 µL samples were loaded onto an agarose gel submerged in TAE buffer with appropriate DNA ladders. DNA electrophoresis was then performed with 100 volts for 45 minutes. Fluorescent bands were visualized using 260 nm ultraviolent radiation in a dark room, and images taken.

GST-protein Expression and Purification

Once enough amplified pGEX-4T-1 was obtained, 3µL of 0.05 µg/µL was used for the transformation of 50 µL of BL21 E. coli melted on ice in autoclaved tubes. As with the DH5α cells, they were incubated together on ice for 30 minutes, followed by a ten second 42˚C heat shock and further incubation on ice. Finally, LB medium was added. After incubation for 90 minutes in the tube, 100 µL was plated onto LB Amp^+ agar plates, and left in 37˚C overnight. A single BL21 E. coli colony was selected, and used to inoculate a sterile tube with LB medium. As with DH5α cells, they had to be grown gradually in a stepwise fashion over days, scaling up the overall biomass of E. coli containing the plasmids of interest. Ampicillin resistance was continuously selected for by the consistent addition of ampicillin whenever LB medium was

used for culturing. Addition was done prior to inoculation with bacterial culture, but after autoclaving (to prevent denaturation/inactivation of the antibiotic). Aseptic technique was always utilized to prevent any opportunity for contamination. The day prior to the induction of protein expression, Amp^+ YTC medium (a more nutritious version of LB medium) was inoculated with the growing culture, and left overnight for less than 14 hours. The timing was crucial, as induction of the lac operon must occur while the BL21 E. coli are still in the logarithmic growth phase of their growth curve. This was determined by spectrophotometric analysis of the A_{600}, (absorbance at λ=600 nm as measured by the Ultrospec 2100 pro spectrophotometer), which had to be between 0.5 and 1.0. When the correct absorbance was measured, and thus an appropriate concentration of cells present, isopropyl β-D-1-thiogalactopyranoside (IPTG, for lac operon induction, thus expressing the plasmid, with production of the fusion protein) was added to a final concentration of 1 mM, and incubation at 37˚C with 250 rpm shaking was continued for the next five hours. After the incubation period was over, the E. coli cells were centrifuged into pellets with 5000 g for 15 minutes, suspended with B-PER (i.e. bacterial protein extraction reagent) to lyse the cells, and incubated at room temperature for 20 minutes. Centrifugation at 15000 g now took place for 15 minutes, and the supernatant (with protein from lysed cells) was transferred to a fresh tube, ready for GST-tagged protein purification (GST is glutathione S-transferase).

To purify any GST-tagged proteins produced, GE Glutathione Sepharose 4B beads were used. The original 75% slurry in ethanol had to first be centrifuged in order to remove the solvent, and rinsed several times with PBS, centrifuging and removing the solvent each time. When centrifuged, 500 g X 5 minutes was sufficient. The beads were finally brought to a final slurry concentration of 50% in PBS. 400 µL of this prepared slurry was added to the 10 mL tubes of supernatant with extracted protein, and incubated for one hour at room temperature with gentle agitation. The supernatant was removed and frozen in case unbound GST target proteins remained. The beads (bound tightly to the GST-proteins) were then washed three times with 2 mL of PBS; suspending, centrifuging, and removing/discarding the supernatants each time. Finally, 400 µL of the Glutathione Elution Buffer (containing reduced glutathione, to cleave off the proteins from the beads) was added, incubated at room temperature for 20 minutes, centrifuged, and the supernatant collected in a tube for analysis. Elution was performed twice more for a total of three rinses and tubes of liberated fusion proteins. Finally, as glutathione is a tripeptide itself, and in excess in the elution buffer, a protein assay inappropriately gave high false positives for protein concentration in all of the tubes. Hence, ultraviolent absorbance (at λ=280 nm) of the samples was measured (and control glutathione elution buffer) in a 96 well plate by a VICTOR^3 1420 Multilabel Counter spectrophotometer. This was because A_{280} is known to be a good estimate for GST fusion protein concentration[23].

Mitochondrial Isolation and Treatment

Mitochondria were obtained from the livers of wild type rats and mice in accordance with the protocol guidelines of the Canadian Council on Animal Care and approved by the University of Manitoba Animal Care Ethics committee. Immediately after the sacrifice of the animal, the livers were harvested, and 0.5 g of minced tissue was rinsed with PBS prior to being homogenized with an all-glass dounce homogenizator in 2 mL of Ice-cold Isolation buffer. The homogenates were centrifuged at 2000 g for three minutes, with the supernatants transferred to new tubes and then

centrifuged at 10000 g for 10 minutes, thereby concentrating the mitochondria within the supernatants into pellets. These pellets were then washed once, and resuspended within washing/respiration buffer at a concentration of about 10 mg/mL (as determined by "Bio-Rad protein assay dye"), and distributed into several Eppendorf tubes. Depending on which trials were being run, each tube was then treated for 15 minutes with prospective VDAC inhibitors (see Table 2) such as Dextran T70, König's polyanion, Ruthenium Red, phosphorothioate oligonucleotide 18-mer randomers, or nothing (as a control). Following this, either nothing (true control), GST protein (control for GST tag itself), GST-BNIP3, or GST-BNIP3ΔTM (BNIP3 without its transmembrane domain), were incubated with the mitochondrial suspensions. As previously mentioned, countless pilot studies optimizing ideal concentrations for both proteins and inhibitors were completed. Incubation with the fusion proteins were done for several time periods (0.5, 1, 1.5, and 2 hour incubations) at varying temperatures (0˚C, 20˚C, and 37˚C) and concentrations (0.1μM, 0.5μM, 1.0μM, 5μM, and 10μM). Pre-incubation pilot studies with prospective VDAC inhibitors showed S-18 phosphorothioate oligonucleotides to be the best at a concentration of 2.5μM, and fusion protein incubation to be optimal at a working concentration of 1μM for 30 minutes on ice, and 15 minutes in 37˚C (too much heat prematurely destroys the mitochondria, too little and the incubation effect is not seen). Incubation with inhibitors was always performed on ice to preserve the mitochondria, and thoroughly homogenized with the mitochondrial pellets. Rinsing with washing buffer took place between treatments. After fusion protein incubation with the mitochondria and centrifugation (12000 g for 10 minutes), the supernatants were collected for analysis of Endo G/AIF release, and the pellets resuspended in 0.1M $Na_2CO_{3(aq)}$ for 20 minutes on ice (remove unbound BNIP3). Centrifugation took place again at 21000 g for 15 minutes, with two more rinse/centrifugation cycles with washing buffer to further rinse off any excess GST-BNIP3 proteins. All of these samples, both mitochondrial pellet and supernatant sets were now ready for Western Blot analysis.

Western Blot

All samples from the aforementioned trials were boiled for five minutes in lysis/loading buffer (4:1 ratio). Bio-Rad apparatus was used in preparation of the gel, with 4 mL of separating gel poured in first, followed by distilled water. When polymerisation was complete, the water was removed and replaced with stacking gel and a 10-well comb. Once set, running buffer was added, and 10 μL of sample loaded into each well and Western Blot began running at 80 volts. After the samples reached the separating gel, 120 volts was applied until completion of the blot (once the dye reached the bottom of the gel). Protein assays were done routinely to ensure appropriate sample quantities were being loaded. The separating gels and Hybond-P PVDF membranes (Amersham Biosciences) were cut down to size and equilibrated in transfer buffer for ten minutes prior to assembly of the standard transfer cassette apparatus (with sponges, filter paper, gel and PVDF membrane sandwiched in the middle). The PVDF was first activated in 100% methanol before being put in the transfer buffer. The transfer was performed at 180 mA for two hours in ice. After transferring, Ponseau S staining was performed to ensure a good transfer, followed by blocking with 5% milk in TBS-T for 20 minutes. Subsequent incubation with 1˚ monoclonal antibodies in 5% milk (approx. 1:1000 dilutions) was done for BNIP3, EndoG, AIF, VDAC, Cox4, and GST proteins as needed overnight with mild agitation at 4˚C. After thoroughly rinsing the membranes with TBS-T several times, they were incubated with appropriate 2˚ (1:3000 solutions) anti-rabbit/goat antibodies at room temperature for an hour.

After further rinsing (3X15 minutes in TBS-T), the membranes were reacted with ECL Plus kit reagents (PerkinElmer), in order to induce luminol-based chemiluminescence upon exposure to horseradish peroxidise (on the 2˚ antibodies). Autoradiography was then done in the dark room with X-ray film overlaying the membranes in a film cassette for various exposure times, prior to being developed for further analysis.

ROS (Reactive Oxygen Species) Assay Analysis

After mitochondrial incubation and treatment, 25 µL samples were mixed with 25 µL of 40 µM dichlorofluorescein diacetate (DCFDA) in HBSS, for a working concentration of 20 µM in 96 well plates. Controls for DCFDA and samples on their own were performed. The plate was incubated in 37˚C for half an hour, and spectrofluorometry was performed on a VICTOR^3 1420 Multilabel Counter with an excitation λ of 485 nm and an emission λ of 535 nm. Raw data in A_{535} was ready for statistical analysis.

Measurement of Mitochondrial Membrane Potential ($\Delta\psi_m$)

$\Delta\psi_m$ is the value for the mitochondrial membrane potential, an index of the cation gradient across the inner mitochondrial membrane. It is responsible for the maintenance of the proton circuit down its gradient resulting in ATP production, and thus is an excellent method of determining mitochondrial functionality after a given treatment. Mitochondrial pellets were incubated with 5µM tetramethylrhodamine, and spectrofluorometry was performed in order to determine the $\Delta\psi_m$, using a VICTOR^3 1420 Multilabel Counter at an excitation wavelength of 553 nm, and emission at 576 nm.

Densitometry and Data Analysis

Quantitative Western Blot densitometric analysis was done with "Quantity One", a basic densitometry program. Microsoft Excel was then used for the statistical significance analysis (i.e. determining the p-value, etc.) Membranes chosen for statistical analysis in this project were selected through the rigorous application of key unifying parameters, such as those with the lowest background exposure, sharpest borders in the blots, and best contrast between different groups (as many under/overexposed membranes would underestimate the statistically relevant difference between bands on individual blots). Unfortunately, due to the variance of the limited preliminary data, and inability to compare data between separate blots (different baseline exposures), there was not a sufficient quantity to appropriately apply a t-test or ANOVA analysis. These will be done as more complete data arrives in the near future.

Results

Although SY5Y culturing was useful in showing the trend of increased EndoG release and BNIP3 dimerization (in the nuclear fraction) over time after an episode of hypoxic stress (Fig. 2), growing the cells proved to be an impractical method of obtaining adequate mitochondrial mass for the fusion protein incubation experiments. This is clear evidence for the delayed apoptosis

phenomenon previously discussed caused by BNIP3. Thus a method of freshly sacrificed, live animal source mitochondria would be required.

After a summer of optimizing all of the experimental conditions, it was concluded that the GST-fusion proteins were bad, producing nonspecific bands everywhere, and strange, consistently unreliable bands upon autoradiography. The ΔTM protein appeared to have more protein than regular BNIP3, as a solid line of nonspecific bands was often observed with several 1˚ antibodies. Unbelievably, what appeared as AIF bands was found in the pure ΔTM protein fraction itself, and BNIP3 bands were missing from the BNIP3 pure protein fraction. From the perspective of fusion protein incubation, no reliable conclusions could be drawn, other than some kind of degradation or contamination had occurred, and the samples would need to be replaced the following summer. The VDAC inhibitors all had problems of their own, appearing unreliable and random in their effects. Dextran proved to be too thick for practical use, as the supernatant could not be removed due to its viscosity. When removed carefully, inhibition was shown to be unreliable. Despite the explosive fragility of the synthesis reaction, once synthesized, König's polyanion was uneventful for AIF, and unreliably effective for EndoG. Ruthenium Red had stark inhibition of both EndoG and AIF, but made everything faint for those columns (implying it's binding to the proteins); the mitochondrial pellet was strongly stained, and the ruthenium red could not be rinsed off despite many attempts. The S-18 randomers were inconclusive, as they came at the end of the summer, and only one trial was done.

Although tedious, the transformation, and successful culturing of both the DH5α and BL21 E. coli was relatively uneventful. Plasmid concentrations were 0.03 and 0.04 μg/μL, and after cleaving with BamHI and NotI restriction endonucleases, two DNA fragments were fluorescing under ultraviolet light, and only one in the control; thus reassuring us the plasmids were indeed functional. Using A_{280} as an estimate, the old, defective proteins were being estimated at a concentration of 0.79 mg/mL (BNIP3) and 0.81 mg/mL (ΔTM), and the newly synthesized ones at 0.77 mg/mL (BNIP3) and 0.78 mg/mL (ΔTM). The new protein solutions thus had concentrations of 17 μM and 18 μM respectively, with room for dilution when incubating experiments.

After several pilot studies, optimal conditions for this experiment were determined to be 0˚C, for 30 min., followed by 37˚C for 15 min.; with a final fusion protein concentration of 2 μM in respiration buffer (containing a mitochondrial mass of 10 mg/mL). If necessary, VDAC inhibition should be done with S-18 randomers at 0˚C for 15 minutes with a working concentration of just over 1 μM.

When the final rounds of experiments were run with the freshly synthesized GST fusion proteins and optimized conditions, several interesting and statistically significant phenomena were noticed. For instance, there was a mean of a (1.60 ± 0.36) – fold difference between the BNIP3-incubated with/without VDAC inhibition groups, with inhibition always being lower. With a p-value < 0.05, this is a statistically significant result, confirming our hypothesis. The same phenomenon was observed with the truncated BNIP3ΔTM, with the VDAC inhibition-lacking group having a (1.22 ± 0.10)-fold increase above the comparable one with inhibition. Interestingly enough, if one looks at the two values, although not enough data has been collected for statistical significance, the VDAC inhibition effect is more pronounced with the un-truncated

whole BNIP3 protein. Finally, although a lack of sufficient data prevents extensive analysis for BNIP3ΔTM's effect on AIF release, BNIP3 groups with and without prior VDAC inhibition had a (1.51±0.20)-fold difference in AIF release. See Figures 4 and 5 for Western Blot images showing the aforementioned differences; Table 3 for sample statistical calculations; and Figure 6 for a graphical representation detailing the magnitude of difference in AIF/EndoG release between different protein ± VDAC inhibition groups.

ROS analysis was rather inconsistent in values between groups, but one trend was definitely observed within individual studies. That is, ROS formation was consistently less when VDAC inhibition was present, with preliminary statistical analysis showing a (1.30 ± 0.08)-fold and (1.71 ± 0.09)-fold difference between the BNIP3 groups (3 separate experiments were used in the collection of those mean data), and a (1.24 ± 0.08)-fold difference in the ΔTM groups. Evidently, further quantification, statistical analysis, consistency, and subsequently greater statistical significance, is necessary for relevant and meaningful analysis in the future. $\Delta\psi_m$ was still being processed with further replication needed (as do most of the aforementioned results) at the time of publishing. The results of data processing and analysis done so far have been discussed throughout the results where relevant, and can be seen in Figs. 4,5, and 6.

Discussion

Although it is virtually impossible to know everything that went wrong in the first summer of this project, one thing manifested itself as being certainly clear – the fusion proteins were four years old. Synthesized in 2008, I can only begin to imagine what kinds of degradative processes or contaminative mishaps may have occurred throughout that time period. Despite theoretically having nothing wrong with them, it is clear that many of the ambiguous and random results obtained can be deemed a direct result of defective proteins. As for the VDAC inhibitors, to be fair, it is difficult to differentiate inhibitor issues from those the old fusion proteins, however, due to practical reasons, both König's polyanion and dextrose were eliminated from the VDAC inhibitor arsenal. After extensive literature research, it was found that phosphorothioate oligonucleotides are by far more specific and potent inhibitors of VDAC channels as compared to traditional agents such as König's polyanion and dextrose[15] anyway. Upon closer analysis, Ruthenium Red cleared everything everywhere on the Western Blots. It is hypothesized that the impractical separation of ruthenium red from the mitochondria resulted in binding of any proteins that would otherwise have been detected in the mitochondrial pellet or released into the supernatant, which made it useless for our purposes (despite yielding fabulous "inhibitory" results). With the optimization trials, it became evident that phosphorothioate 18-mer oligonucleotides could indeed be used successfully for VDAC inhibition, and the literature supported this. As for the incubation, it was found that longer periods of time at warmer temperatures began to degrade the proteins, and artificially destroy the mitochondria. Too short a time period, especially when on ice, was shown to inhibit the actual interaction of the fusion proteins with the mitochondria during the incubation. Thus an optimal balance was reached as described in the results.

Once the final successful preliminary results were in, it was four days prior to the due date of this publication, so there was not sufficient data to perform extensive statistical analyses with large n

values. Despite the fact that more replication is required, as well as further analysis looking at other related parameters, such as $\Delta\psi_m$ assays; statistically significant results were certainly obtained, and their effects can be discussed. The fact that VDAC inhibition prevents EndoG and AIF release (at least for BNIP3) indicates that VDAC is somehow functionally important in translating BNIP3's apoptogenic message into the mitochondria. This data strongly supports our hypothesis concerning the nature of BNIP3 and VDAC interactions. Although admittedly too early to tell, the fact that BNIP3ΔTM also experiences inhibition implies that it too is active, which could imply that the transmembrane domain is not the one through which the response is mediated. Alternatively, the fact that VDAC inhibition has significantly less of an effect on preventing EndoG/AIF release could indicate that the lack of a transmembrane domain is not really in fact binding to VDAC in the same way as unaltered BNIP3. Finally, although the experimental ROS release data is still extremely premature, it indicates decreased ROS production upon VDAC inhibition, which further supports our hypothesis, and can be used as confirmation that VDAC is in fact involved with ROS production and release from mitochondria in BNIP3-mediated apoptosis. In the future, further determination/confirmation of GST fusion protein concentrations (among other parameters) using more reliable methods would prove to be useful, as well as ROS and $\Delta\psi_m$ studies, and further replication of those already done. Different plasmids with specific amino acid mutations will be used to specifically pinpoint the locations at which BNIP3 is interacting with VDAC, and further in vivo VDAC inhibition/BNIP3-knockout models in mice will be studied in greater detail. Depending on those results, there are several further exciting directions in which this project can be taken in the future.

Conclusion

In conclusion, much work remains to be done, and several questions remain elusively unanswered. However, it is safe to conclude that there is definitely a statistically significant decrease in apoptogenic mitochondrial protein release into the cytosol upon VDAC inhibition and BNIP3 incubation, which if sufficiently replicated, proves that BNIP3 translates its apoptotic caspase-independent cascade into the mitochondria through its noncoincidental interaction(s) with VDAC, as first suggested by our hypothesis.

References

1. Love S. Apoptosis and brain ischaemia. Progress in Neuro-Psychopharmacology and Biological Psychiatry. 2003; 27:267-282.
2. Zhang Z., Yang X., Zhang S., Ma X., Kong J. BNIP3 Upregulation and EndoG Translocation in Delayed Neuronal Death in Stroke and Hypoxia. Stroke. 2007; 38:1606-1613.
3. Cho B. B., Toledo-Pereyra L. H. Caspase-Independent Programmed Cell Death Following Ischemic Stroke. Journal of Investigative Surgery. 2008; 21: 141-147.
4.Weng J., Kong J. Delayed Neuronal Death in Stroke: Molecular Pathways. Advancements in Neurological Research. 2008; 1-21.
5. Shoshan-Barmatz V., De Pinto V., Zweckstetter M., Raviv Z., Keinan N., Arbel N. VDAC, a mutli-functional mitochondrial protein regulating cell life and death. Molecular Aspects of Medicine. 2010; 31: 227-285.
6. Kinnally K. W., Peixoto P. M., Ryu S-Y., Dejean L. M. Is mPTP the gatekeeper for necrosis, apoptosis, or both? Biochimica et Biophysica Acta. 2010; 1813:616-622.
7. Xu X., Chua C. C., Kong J., Kostrzewa R. M., Kumaraguru U., Hamdy R. C., Chua B. H. L. Necrostatin-1 protects against glutamate-induced glutathione depletion and caspase-independent cell death in HT-22 cells. Journal of Neurochemistry. 2007; 103: 2004-2014.
8. Krasnikov B. F., Melik-Nubarov N. S., Zorova L. D., Kuzminova A. E., Isaev N. K., Cooper A. JL., Zorov D. B. Synthetic and natural polyanions induce cytochrome c release from mitochondria in vitro and in situ. Am J Physiol Cell Physiol. 2011; 300:C1193-C1203.
9. König T., Stipani I., Horvàth I., Palmieri F. Inhibition of Mitochondrial Substrate Anion Translocators by a Synthetic Amphipathic Polyanion. Journal of Bioenergetics and Biomembranes. 1982; 14:297-305.
10. Scharstuhl A., Mutsaers H. A. M., Pennings S. W. C., Russel F. G. M., Wagener F. A. D. T. G. Involvement of VDAC, Bax, and Ceramides in the Efflux of AIF from Mitochondria during Curcumin-Induced Apoptosis. PLoS ONE. 2009; 4(8):e6688.
11. König T., Kocsis B., Mézáros L., Nahm K., Zoltán S., Horvàth I. Interaction of a synthetic polyanion with rat liver mitochondria. Biochimica et Biophysica Acta. 1977; 462:380-389.
12. Colombini M., Yeung C. L., Tung J., König T. The mitochondrial outer membrane channel, VDAC, is regulated by a synthetic polyanion. Biochimica et Biophysica Acta. 1987; 905:279-286.
13. Gellerich F. N., Kapischke M., Kunz W., Neumann W., Kuznetsov A., Brdiczka D., Nicolay K. The Influence of the cytosolic oncotic pressure on the permeability of the mitochondrial outer membrane for ADP: implications for the kinetic properties of mitochondrial creatine kinase and for ADP channelling into the intermembrane space. Molecular and Cellular Biochemistry. 1994; 133/134:85-104.
14. Stein C. A., Colombini M. Specific VDAC Inhibitors: Phosphorothioate Oligonucleotides. J Bioenerg Biomembr. (2008) doi: 10.1007/s10863-008-9139-9.
15. Tan W., Loke Y-H., Stein C. A., Miller P., Colombini M. Phosphorothioate Oligonucleotides Block the VDAC Channel. Biophysical Journal. 2007; 93:1184-1191.
16. Chinnadurai G., Vijayalingram S., Gibson S. B. BNIP3 subfamily BH3-only proteins – mitochondrial stress sensors in normal and pathological functions. Oncogene. 2008; 27:114-227.
17. Moore C. L. Specific Inhibition of Mitochondrial Ca^{++} Transport by Ruthenium Red. Biochemical and Biophysical Research Communications. 1971; 42(2):298-305

18. Israelson A., Zaid H., Abu-Hamad S., Nahon E., Shoshan-Barmatz V. Mapping the ruthenium red-binding site of the voltage-dependent anion channel-1. Cell Calcium. 2008; 43:196-204.
19. Rostovtseva T., Colombini M. VDAC Channels Mediate and Gate the Flow of ATP: Implications for the Regulatino of Mitochondrial Function. Biophysical Journal. 1997; 72:1954-1962.
20. Schild L., Keilhoff G., Augustin W., Reiser G., Striggow F. Distinct Ca^{2+} thresholds determine cytochrome c release or permeability transition pore opening in brain mitochondria. The FASEB Journal. 2001; 15:565-578.
21. De Pinto V., Messina A., Lane D. J. R., Lawen A. Voltage-dependent anion-selective channel (VDAC) in the plasma membrane. FEBS Letters. 2010; 584:1793-1799.
22. Shoshan-Barmatz V., Ben-Hail, D. VDAC, a multi-functional mitochondrial protein as a pharmacological target. Mitochondrion. (2011) doi: 10.1016/j.mito.2011.04.001
23. Smith D.B., and Johnson KS. Single-step purification of polypeptides expressed in Escherichia coli: Schistosoma japonicum glutathione S-transferase. Gene. 1988; 67 (31).
24. Baines CP, Kaiser RA, Sheiko T., Craigen WJ, and Molkentin JD. Voltage-Dependent Anion Channels are Dispensible for Mitochondrial-Dependent Cell Death. Nat Cell Bio. 2007; 9:(5).

Tables and Figures

Table 1. Solutions used in these experiments.

Separating Gel ddH_2O – 3.3 mL 30% acrylamide – 4.0 mL 1.5M Tris-HCl (pH in ddH_2O) – 2.5 mL 10% SDS – 0.1 mL 10% APS – 0.1 mL TEMED – 0.010 mL	**Stacking Gel** ddH_2O – 3.4 mL 30% acrylamide – 0.83 mL 1.0M Tris-HCl (pH 6.8 in ddH_2O) – 0.63 mL 10% SDS – 0.05 mL 10% APS (Ammonium Persulphate) – 0.05 mL TEMED – 0.005 mL
TBS Tris (Fisher) – 3.025g Glycine (Fisher) – 18.8g SDS ("Sodium Dodecylsulphate", Fisher) – 1g Use ddH_2O to bring volume up to 1L.	**PBS** NaCl – 8g KCl – 0.2g Na_2HPO_4 – 1.15g KH_2PO_4 – 0.2g Use ddH_2O to bring volume up to 1 L.
Running Buffer Tris – 15.1g Glycine – 94g 10% SDS – 50 mL Bring volume up to 1L with ddH_2O.	**Ice-cold Isolation Buffer** 320 mM sucrose 1 mM EGTA 10 mM Tris-HCl pH 7.4
Transferring Buffer Glycine – 2.9g Tris – 2.8g Methanol – 200 mL Bring volume up to 1L with ddH_2O.	**Washing/Respiration Buffer** 0.2M sucrose 20mM HEPES pH 7.2 0.1 mM EGTA 4 mM KH_2PO_4
TBS-T TBS – 497.5 mL 20% Tween-20 – 2.5 mL	**0.1 M $Na_2CO_{3(aq)}$** 1.325g Na_2CO_3 ddH_2O – 125 mL
Lysis/Loading Buffer 1M Tris-HCl (pH 6.8 in ddH_2O) – 0.12mL 10% Glycerol – 5 mL 10% SDS – 0.4 mL β-mercaptoethanol – 0.1 mL 1% bromophenol blue – 0.2 mL ddH_2O – 4.18 mL; =**Loading Buffer** (5% protease inhibitor cocktail in RIPA =**Lysis buffer**)	**König's Polyanion** - methacrylic acid - maleic acid anhydride - styrene 1:2:3 molar ratios respectively; all in 33 mL toluene, with 0.18 g of benzoyl peroxide as a catalyst. 60˚C air bath initially, left overnight at 51˚C for 18 hours; 0.18 g of thick, gummy yellow residue collected the next morning. Prepared[8,9,11,12] with KOH in ddH_2O, titrated to pH 7.2
Hypoxic Chamber 1.5% O_2 5% CO_2 93.5% N_2	**Complete DMEM Medium** Invitrogen "Dulbecco's Modified Eagle Medium" powder in ddH_2O, + 2mM L-glutamine, 10% FBS, and 1% polymycin, neomycin, streptomycin
EBSS solution Invitrogen "Earle's Balanced Salt Solution" powder in ddH_2O	**Ponseau S Reagent** .25% Ponseau 5% acetic acid in ddH_2O
HBSS (Ca^{2+} and Mg^{2+} free) KCl – .04 g/L KH_2PO_4 – .06 g/L NaCl – 8.0 g/L $NaHCO_3$ – .35 g/L Na_2HPO_4 – .048 g/L HEPES – 5.96 g/L D-glucose – 1.00 $g_{/L}$	**TAE/Agarose Gel** 1.0 mL 0.5M EDTA pH 8.0 0.572 mL CH_3OOH 2.42 g. Tris Add ddH_2O until 500 mL Dissolve (1% w/v) 5 g of agarose, and heat to a boil twice; until fully dissolved. Pour Electrophoresis Gel.
YTC Medium Tryptone – 16 g/L Yeast Extract – 10 g/L NaCl – 5 g/L	**LB Medium/Plates** Tryptone – 8 g/L Yeast Extract – 5 g/L NaCl – 5 g/L Add 15 g/L agar and autoclave, prior to pouring into plates.
Glutathione Elution Buffer 0.154 g. reduced glutathione dissolved in 50 mL of 50 mM Tris-HCl ddH_2O, pH 8.0	**50% Glutathione Sepharose 4B Slurry** 1 mL PBS/mL bead bed volume

Table 2. VDAC Inhibitors, Mechanisms of action, and Ideal concentrations, respectively in columns. Inhibitors used already are bolded.

Cyclosporin A[6,10]	Binds cyclophilin D, and stops mPTP from opening. CycD is known activator/regulator of mPTP, but prob not part of mPTP; inhibits calcineurin	2.5 μM
Bongkrekic Acid[6]	Locks ANT in opposite conformation, preventing mitochondrial permeability transition; atractyloside also ANT inhibitor, induces MPT. ANT not only inner membrane bridge – also prevents mitochondrial depolarization, permeability, and rupture.	1 mg/mL, .01M in Tris
DIDS[5,10]	Binds non-selectively to anion exchangers, prevents Bax activation of VDAC, not through mPTP pore, but probably something else; decreases conductance of VDAC reconstituted into a planar lipid bilayer.	500 μM for apoptosis inhibition
König's polyanion[9,11, 12]	Induces VDAC closure, and low conductance state. Might act through hydrophobic interactions, not just electrostatically like dextran sulphate. Has been shown to block Cyto c release through functional mitochondrial pore, but also enhances mitochondrial swelling and Cyto c release.	1 – 4 μM, 50 μg/mL = 5μM, MM = 10 kDa
Dextran 70 (Dextran sulphate)[13,14, 19,20]	Polyanion, works just like König's. Apparently 500 kDa dextran sulphate "works very well". Found to be dependent on mass (w/v), REGARDLESS of molecular weight. Dramatically increases the probability that VDAC will close at lower voltages. Prevents transport of molecules through outer membrane via VDAC.	10% w/v, MM = 70 kDa (>15% start having problems with respiration)
Ruthenium Red[5,17,18]	Specifically binds to several Ca^{++} uniporter proteins, decreasing Ca^{++} conductance of bilayer reconstituted VDAC, stabilizing a completely closed state. Prevents Ca^{++} induced apoptosis, and appears to have a direct interaction with VDAC (cytosolic loops 1 and 3). <2.6 mM not enough, 12 mM totally inhibits, 6 mM probably best for decreasing Ca^{++} respiration	0.35 μM/mg of mitochondria; 6 mM in H_2O
G3139 and **phosphothiorate oligonucleotide 18-mer randomers[14,15]**	Probably embeds itself within VDAC as opposed to mere electrostatic mechanism of comparable polyanions ***blockage dependent upon phosphothiorate BACKBONE, NOT sequence; AND these are the most VDAC-specific blockers available to date*** (randomers kept in 10 mM Tris, 1mM EDTA solution for storage)	10 μM, 1 μM best for VDAC specificity; 20μM = Ca^{++} release
VDAC antibodies[21]	Binds to most antigenic region, first 11 N-term amino acids of VDAC; essentially complete block of VDAC	typical 1:2000 antibody dilution

Table 3. Sample calculations for determining the (1.60±0.36) – fold decrease in Endo G release with VDAC inhibition, when incubating mitochondria with BNIP3.

	Adjusted Densitometric Value for BNIP3 treatment	Adjusted Densitometric Value for BNIP3+Inhibitor treatment	Fold Difference
Experiment 1	978	597	978/597= 1.64 fold
Experiment 2	3768	2149	3768/2149= 1.75 fold
Experiment 3	866	617	866/617= 1.40 fold

For a p-value of <0.05 and statistical significance, $= \mu \pm 2s = (1.64+1.75+1.40)/3 \pm 2\,[(\Sigma (x-\mu)^2)/(3-1)]^{0.5}$ = **1.60 ± 0.36**

Figure 1. Caspase-independent apoptotic pathways; including BNIP3 dimerization stimulating AIF/Endo G release (on left). VDAC's proposed role within the mPTP pore (on right, sciencedirect.com).

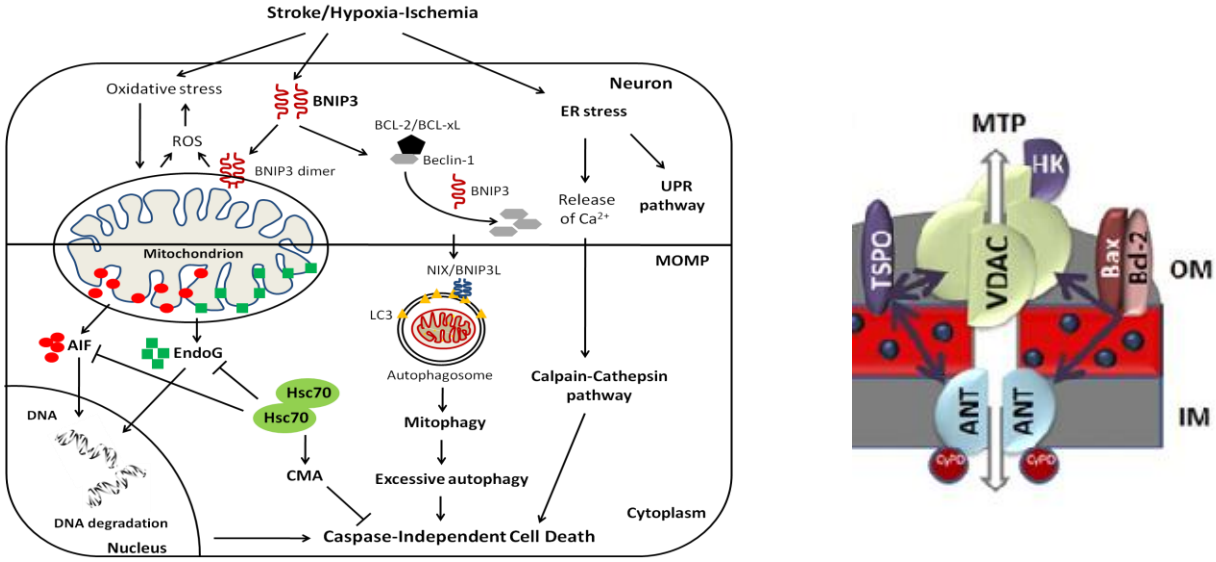

Figure 2. Left; Endo G release increases with time after OGD. Right; BNIP3 dimer increases progressively in nuclear fraction after OGD treatment. Bottom; BNIP3 domain locations.

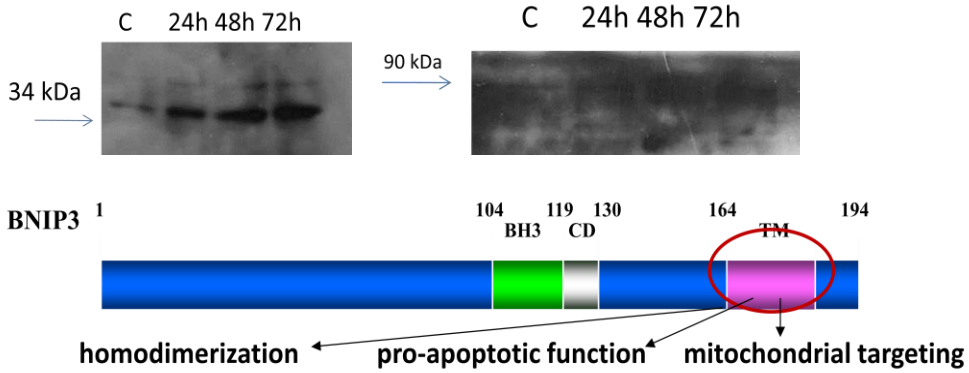

Figure 3. The pGEX-4T-1 plasmid used for the production of GST fusion proteins (GST-BNIP3 and GST-BNIP3TM); the large arrow points out the location into which my genes of interest were spliced.

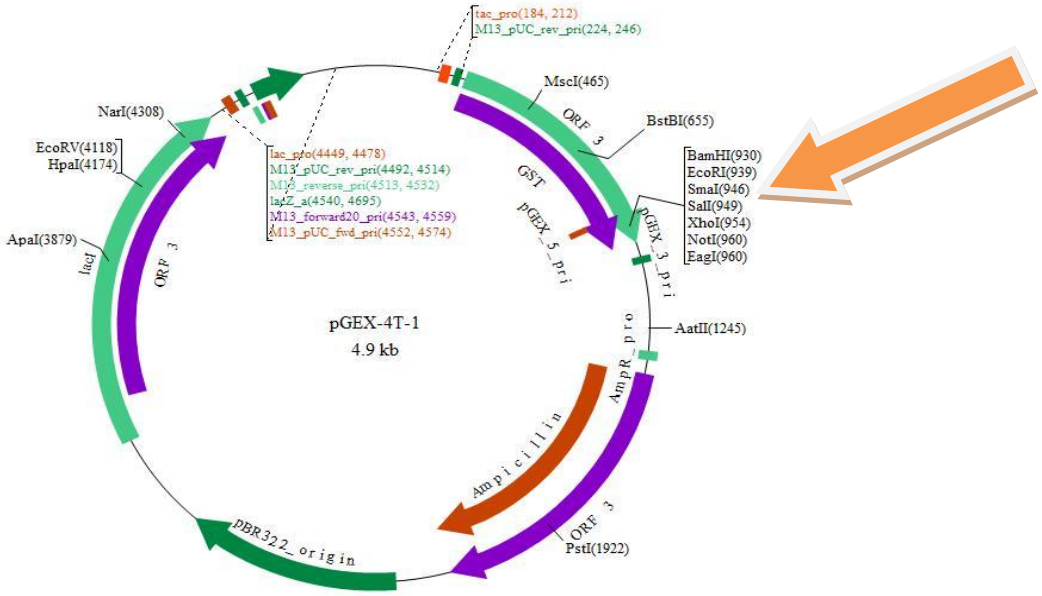

Figure 4. Left; control mitochondria released less EndoG than those incubated with protein. Right; BNIP3-incubated mitochondria released less EndoG when inhibited by an S-18 randomer.

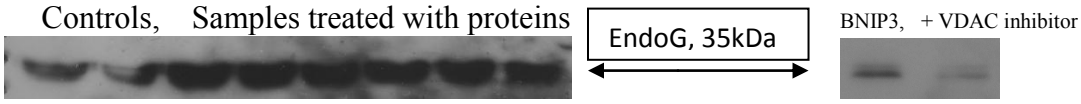

Figure 5. Left; BNIP3ΔTM treated mitochondria release less EndoG when inhibited by an S-18 randomer. Right; BNIP3 releases less AIF when inhibited by an S-18 randomer.

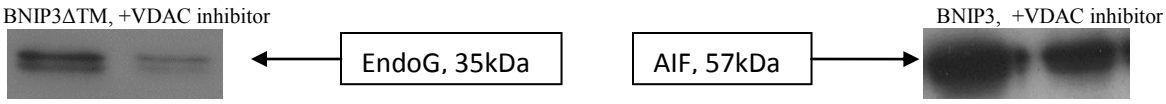

Figure 6. Graphical Representation of Differences between ±VDAC inhibitor-treated groups.